Ultrasonics 57 (2015) 135–143

Contents lists available at ScienceDirect

Ultrasonics

journal homepage: www.elsevier.com/locate/ultras

Fundamental understanding of wave generation and reception using d_{36} type piezoelectric transducers

Wensong Zhou [a,b,*], Hui Li [a,b], Fuh-Gwo Yuan [c,d,*]

[a] Key Lab of Structures Dynamic Behavior and Control of the Ministry of Education, Harbin Institute of Technology, Harbin 150090, China
[b] School of Civil Engineering, Harbin Institute of Technology, Harbin 150090, China
[c] Department of Mechanical and Aerospace Engineering, North Carolina State University, Raleigh, NC 27695, USA
[d] College of Mechanical and Vehicle Engineering, Hunan University, Changsha 410082, China

ARTICLE INFO

Article history:
Received 16 January 2014
Received in revised form 5 November 2014
Accepted 6 November 2014
Available online 15 November 2014

Keywords:
Piezoelectric wafer
d_{36} type
Shear horizontal wave
Frequency tuning
Actuator and sensor

ABSTRACT

A new piezoelectric wafer made from a PMN–PT single crystal with dominant piezoelectric coefficient d_{36} is proposed to generate and detect guided waves on isotropic plates. The in-plane shear coupled with electric field arising from the piezoelectric coefficient is not usually present for conventional piezoelectric wafers, such as lead zirconate titanate (PZT). The direct piezoelectric effect of coefficient d_{36} indicates that under external in-plane shear stress the charge is induced on a face perpendicular to the poled z-direction. On thin plates, this type of piezoelectric wafer will generate shear horizontal (SH) waves in two orthogonal wave propagation directions as well as two Lamb wave modes in other wave propagation directions. Finite element analyses are employed to explore the wave disturbance in terms of time-varying displacements excited by the d_{36} wafer in different directions of wave propagation to understand all the guided wave modes accurately. Experiments are conducted to examine the voltage responses received by this type of wafer, and also investigate results of tuning frequency and effects of d_{31} piezoelectric coefficient, which is intentionally ignored in the finite element analysis. All results demonstrate the main features and utility of proposed d_{36} piezoelectric wafer for guided wave generation and detection in structural health monitoring.

1. Introduction

Ultrasonic guided waves are being used extensively for effectively detecting the damage in structural health monitoring (SHM) [1,2]. The guided waves reflect, transmit or scatter, often with additional converted wave modes when they encounter discontinuous, such as geometric boundaries, flaws, or damages, therefore methods for damage detection are mainly based on analysis of waveform received by transducers at fairly high ultrasonic frequency range [3,4].

Conventional guided waves include Lamb waves with symmetric and antisymmetric modes, and shear horizontal (SH) waves in thin plate-like structures, while in elongated cylindrical structures like rods, pipes, cable strands or fibers, longitudinal modes wave, flexural modes wave and torsional modes wave propagate along their long axes [5]. For most of wave modes, one of the fundamental characteristics is the existence of dispersion, which gives the nonlinear relationship between wavenumber and frequency. As a consequence, signals with a wide bandwidth will become significantly distorted as the propagation distance or time duration increases and further attenuated in amplitude due to geometric spreading. Therefore, dispersion results in complex signal processing in the application of guided waves based SHM methods.

A narrowband signal in small compact time duration is usually used to generate the guided wave to minimize influence of the dispersion, yet it still prevails for long propagation distances. One of the solutions is to utilize non-dispersive guided wave, such as fundamental shear horizontal (SH_0) waves in thin plates or the first mode torsional waves in cylindrical structures. They are usually generated by a special type of transducers, such as magnetostrictive transducers e.g., [6,7] and thickness shear (d_{15}) mode piezoelectric transducers [8], which can readily generate non-dispersive guided waves. Seung et al. proposed an omni-directional SH wave magnetostrictive patch transducer that consists of an annular magnetostrictive patch [9], a toroidal coil and a permanent magnet. However these techniques require additional confinement

* Corresponding authors at: Key Lab of Structures Dynamic Behavior and Control of the Ministry of Education, Harbin Institute of Technology, Harbin 150090, China (W. Zhou). College of Mechanical and Vehicle Engineering, Hunan University, Changsha 410082, China (F.-G. Yuan).

E-mail addresses: zhouwensong@hit.edu.cn (W. Zhou), yuan@ncsu.edu (F.-G. Yuan).

http://dx.doi.org/10.1016/j.ultras.2014.11.003
0041-624X/

in order to generate such waves, resulting in a larger footprint than miniature piezoelectric wafers, which even can be embedded into the structures.

Another reason leading to complicated waveform is multi-mode of guided waves. For a given frequency, a finite number propagating wave modes will be generated and propagate simultaneously. This issue can be overcame by frequency tuning technique, which is to seek for a specific frequency range to amplify or decrease the amplitude of response with respect to various frequencies for different modes wave respectively [10].

A new piezoelectric wafer has been proposed to generate and detect the SH waves [11]. This preliminary investigation also demonstrated its ability to detect the damage. This special behavior owes to the piezoelectric coefficient d_{36} in its piezoelectric matrix. The direct piezoelectric effect of piezoelectric coefficient d_{36} indicates that under external in-plane shear stress σ_{12}, the charge is induced on a face perpendicular to the poled z-direction. The corresponding converse piezoelectric effect is when the external electric field is applied in the z-direction, the response is the in-plane shear deformation experienced by the material on the face. Toward the practical application, this paper investigates further the directionality and the tuning frequency characteristic of the proposed piezoelectric wafer by simulation and experiments.

2. Brief characteristics of guided waves in plates

For a plate bounded by the surfaces $x_3 = \pm h/2$ and is of infinite extent in the x_1 and x_3 directions, the harmonic wave motion can be divided into two classes of wave motions: plane strain and antiplane shear (or shear horizontal) motions. For harmonic wave motion in plane strain in the (x_1, x_3)-plane of an elastic plate, the guided wave field can be represented by a standing wave in the x_2 direction and a propagating wave in the x_1 direction, which is known as Lamb waves. Lamb waves can be separated into symmetric and antisymmetric modes. One of the most discussed issues is their dispersion property given by:

$$\frac{\omega^4}{c_T^4} = 4k^2q^2\left[1 - \frac{p}{q}\frac{\tan(ph/2+\gamma)}{\tan(qh/2+\gamma)}\right] \tag{1}$$

where ω is angular frequency, c_T is transverse wave velocity, k is wave number, $q = \sqrt{\omega^2/c_T^2 - k^2}$, $p = \sqrt{\omega^2/c_L^2 - k^2}$, h is the thickness of the plate, $\gamma = 0$ and $\pi/2$ represent symmetric and antisymmetric modes, respectively. The dispersion relation results in an infinite number of wave modes defined by S_0, S_1, S_2, ..., A_0, A_1, A_2, ... for symmetric and antisymmetric modes, respectively. The corresponding displacement components for wave modes can be expressed as:

$$\begin{aligned} u &= q\left[\cos(qx_3+\gamma) - \frac{2k^2}{k^2-q^2}\frac{\cos(qh/2+\gamma)}{\cos(ph/2+\gamma)}\cos(px_3+\gamma)\right]B \\ w &= -ik\left[\sin(qx_3+\gamma) + \frac{2pq}{k^2-q^2}\frac{\cos(qh/2+\gamma)}{\cos(ph/2+\gamma)}\sin(px_3+\gamma)\right]B \end{aligned} \tag{2}$$

where u and w are displacement components in x_1 and x_3, respectively. B is a constant. Therefore, for Lamb waves, it only has displacement components u and w, and the displacement components v does not exit.

Another type of guided wave in the plate, SH wave, involves antiplane shear motion. In a plate with surfaces normal to x_3, the wave polarized in the (x_1, x_3)-plane with components u and w is decoupled from the SH wave polarized along x_2 with displacement v alone. Its dispersion relation can be written in an analytical form as:

$$\left(\frac{\omega h}{c_T}\right)^2 = (kh)^2 + (n\pi)^2 \tag{3}$$

where $n = 0, 2, 4, \ldots$ for symmetric modes, and $n = 1, 3, 5, \ldots$ for antisymmetric modes. Different with all modes of Lamb waves and the other modes SH waves, the fundamental mode (SH_0) of SH wave is non-dispersive. The SH waves motion is normal to the direction of propagation, x_1. Its only displacement component v can be written as:

$$v = \begin{cases} B_n \cos\left(\frac{n\pi x_3}{h}\right) (\text{symmetric modes}) \\ A_n \sin\left(\frac{n\pi x_3}{h}\right) (\text{antisymmetric modes}) \end{cases} \tag{4}$$

where A_n and B_n are unknown coefficients. Note that the amplitude of SH modes are independent of frequency and wavenumber. Hence the wave structure of the SH mode does not vary along the entire dispersion curve. This is in contrast to Lamb wave behavior, where the wavefield is a function of the position on the dispersion curve. For SH wave excitation, the shear deformation is necessary for the sensor or actuator working in plane, thus traditional piezoelectric is unable to generate and sense it.

3. d_{36} Type piezoelectric wafers

The most widely used piezoelectric material in most of the transducer and actuator applications is lead zirconate titanate ($PbZr(Ti)O_3$, PZT), a ferroelectric ceramic. When this material is poled, it attains a permanently polarized state. For a small variation in the electric field, it behaves approximately linearly near that state, which can be expressed by the following linear piezoelectric equations:

$$\begin{aligned} \varepsilon_{ij} &= c'_{ijkl}\sigma_{kl} + d_{kij}E_k \\ D_i &= d_{ikl}\sigma_{kl} + \varepsilon^T_{ik}E_k \end{aligned} \tag{5}$$

where ε_{ij} and σ_{kl} are the strain and stress tensors, c'_{ijkl}, $dkij$, and ε^T_{ik} are the inverse elastic, piezoelectric, and dielectric constants, respectively. E_k and D_i are electric field and electric displacement component respectively. The poled piezoelectric ceramic is an orthotropic material with a plane of symmetry whose normal is in the poled direction, so the electric constants matrix has only three independent piezoelectric coefficients, d_{31}, d_{33} and d_{15}. All other coefficients are zero, as following:

$$d_{ij} = \begin{bmatrix} 0 & 0 & 0 & 0 & d_{15} & 0 \\ 0 & 0 & 0 & d_{24} & 0 & 0 \\ d_{31} & d_{32} & d_{33} & 0 & 0 & 0 \end{bmatrix} \tag{6}$$

where $d_{31} = d_{32}$, and $d_{24} = d_{15}$. The piezoelectric wafer made of this piezoelectric ceramic is called d_{31} type piezoelectric wafer in this paper.

The proposed piezoelectric wafer in this paper has five independent coefficients, shown as following:

$$d'_{ij} = \begin{bmatrix} 0 & 0 & 0 & d_{14} & d_{15} & 0 \\ 0 & 0 & 0 & d_{24} & d_{25} & 0 \\ d_{31} & d_{32} & d_{33} & 0 & 0 & d_{36} \end{bmatrix} \tag{7}$$

Table 1
Comparison of deformations induced by d_{31} and d_{36} coefficients.

Piezoelectric coefficient	Deformation	Strain
d_{31}/d_{32}	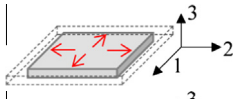	$\varepsilon_1/\varepsilon_2$
d_{36}	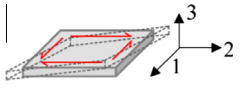	γ_{12}

where $d_{31} = d_{32}$, $d_{14} = d_{25}$, and $d_{24} = d_{15}$. For this wafer, when an external electric field is applied to the wafer in the z direction, the in-plane strain will include not only the normal strain, which induced by d_{31} and d_{32}, but also the shear strain, which is induced by d_{36}. Table 1 lists the detailed difference between these two coefficients.

The proposed piezoelectric wafer may be obtained by means of cutting a type of single crystal, $Pb(Mg_{1/3}Nb_{2/3})O_3$–$PbTiO_3$ (PMN–PT), in a special direction, shown as Fig. 1, in which [h k l] in crystallography denotes a direction and (h k l) a plane orthogonal to the direction [h k l]. The PMN–PT crystal first is orientated in a Cartesian coordinate system with crystal growth direction parallel to z axis. Then the PMN–PT crystal is poled in the [0 1 1] direction, and the wafer is cut in the plane (0 1 1). Zhang et al. [12] gives an example of this piezoelectric constant matrix as following:

$$d'_{ij} = \begin{bmatrix} 0 & 0 & 0 & -696 & 935 & 0 \\ 0 & 0 & 0 & 935 & -696 & 0 \\ -364 & -364 & 890 & 0 & 0 & -1648 \end{bmatrix} \times 10^{-12} C/N \tag{8}$$

where d_{36} is more than four times of d_{31} and d_{32}. Generally, conventional d_{31} type piezoelectric wafer is able to excite Lamb waves (includes A_0 and S_0 modes) on the thin plate. Thanks to the shear deformation induced by d_{36}, the proposed piezoelectric wafer is expected to excite both Lamb waves and shear horizontal waves.

When the piezoelectric wafer is used routinely, the direction of external electric field E is usually along the z-axis and is perpendicular to the surface of the wafer, which is bonded on the surface of plate structure. For the moment, only d_{36} is considered, and then Eq. (5) can be simplified as:

$$\begin{aligned} \sigma_{12} &= \tfrac{E}{1+v}(\varepsilon_{12} - d_{36}E_3) \\ D_3 &= d_{36}\sigma_{12} + \varepsilon_3^T E_3 \end{aligned} \tag{9}$$

For a free d_{36} type piezoelectric wafer without in-plane external electric field and applied stress, the induced in-plane strain by applying a voltage across the z-direction can be expressed as:

$$\varepsilon_{12} = d_{36}E_3 = \frac{d_{36}}{h_p} V_{in} \tag{10}$$

where h_p is the thickness of the wafer. Fig. 1(b) shows the deformation of a d_{36} type piezoelectric wafer placed on the surface of a plate. The deformation can be considered due to a pair of shear strains, γ_{xy} and γ_{yx}. Moreover, the wafer can be equivalent to a group of line force, which is along the four edges of the wafer, applied on the plate. The induced pure shear deformation along the edges results in the guided waves in the plate.

4. Finite element analysis of d_{36} type wafer as actuator and sensor

4.1. Guided waves generation by d_{36} type wafer

Through analyzing the displacement components, different guided wave modes can be understood accurately. Independent displacement components may be extracted naturally from finite element results. In this work, a metallic plate bonded with a d_{36} actuator was modeled with ANSYS to conduct the wave generation and propagation analyses. Fig. 2 shows the aluminum plate with 1.0 mm in thickness, 18 cm in both length and width. With this dimension, all guided waves will be able to prevail and the extensive computation is avoided. The square shaped actuator (4 mm × 4 mm), which is modeled by a Solid5 element in ANSYS, was placed on the location 70 mm away from two nearer edges of the plate. Seven sensing points are positioned on a circle with 60 mm radius around the excitation point with 15° increment. Due to the geometrical symmetry only a quadrant of the circumference is need to capture all guided wave phenomena from the square-shaped actuator located at the center. Displacement components of the sensing point were extracted from the simulation results to explore their variation with respect to different directions. To highlight wave generation using d_{36} type piezoelectric wafer, the relatively small values of piezoelectric coefficients related to the induced in-plane normal deformation are intentionally removed from the piezoelectric material matrix in Eq. (4).

The excitation from the piezoelectric wafer is a 5-cycle sinusoid tone-burst signal enclosed in a Hanning window with a center frequency f_c kept fixed at 160 kHz, since according to results from d_{31} type of PZT, both A_0 and S_0 modes of Lamb waves appear simultaneously under the excitation of this frequency. It can be seen through frequency domain analysis that the frequency components for this narrowband signal are mainly concentrated in a small region around the center frequency f_c, thus the dispersive effect can be significantly reduced. The amplitude spectrum of

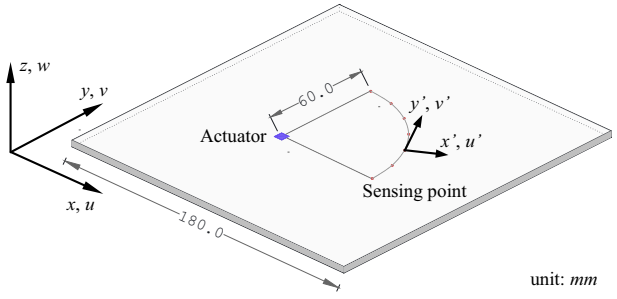

Fig. 2. Layout of the piezoelectric wafer and the sensing point.

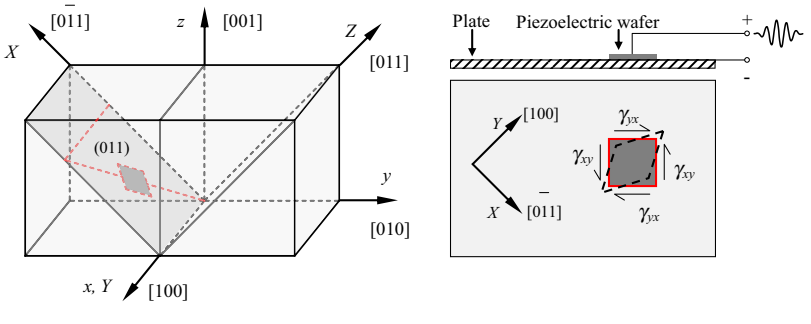

Fig. 1. Cutting direction of poled PMN–PT material and in-plane shear deformation of the PMN–PT mounted on a plate.

excitation signal was plotted together with group velocity dispersion curves corresponding to three wave modes in Fig. 3.

The size of the elements is determined according to the wavelength responding to the lowest phase velocity among A_0, S_0 and SH_0 waves, i.e. the size of elements is less than 1/20 the shortest wavelength, while the time step during finite element analysis is chosen according to the center frequency f_c of excitation signal, i.e. the time step is less than $1/20f_c$.

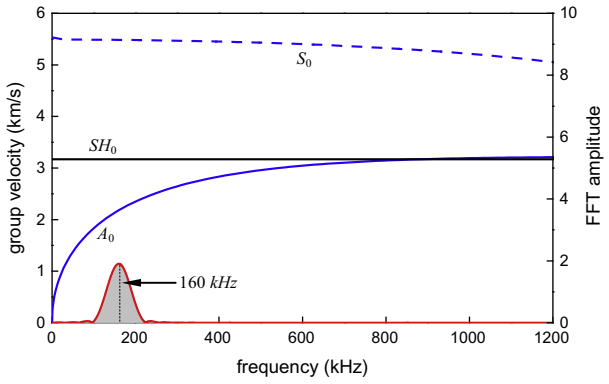

Fig. 3. Group velocity of Lamb wave and amplitude spectrum of excitation signal.

As shown in Fig. 2, for each sensing point, local coordinate (x' and y') is used, in which x' axis is along the radial direction; i.e., the direction of wave propagation. Then, in the local coordinate, all Lamb wave modes should have only two displacement components, u' and w', based on the definition of Lamb wave described in Eq. (2); while the displacement component v' should indicate SH wave described in Eq. (4). Fig. 4 shows the snapshots of the displacement contours on the surface of the plate in three directions, and the total displacement contour, excited by the d_{36} actuator at the time 28 μs respectively. For each figure, the displacement components are transformed to the local cylindrical coordinate, in which the displacement components u' for all nodes are in accordance with the radial direction, and v' the tangential direction. Lamb waves can be identified from Fig. 4(a) and (c) with significant values of u' and w′; while SH wave also can be readily identified in Fig. 4(b). All values in Fig. 4 are extracted, and plotted in Figs. 5 and 6. Fig. 5 shows three displacement components that transform to the local coordinate at the sensing points from 0° to 90°. The range of y axis is kept fixed for illustrating their relative magnitudes. Fig. 5(a) shows three displacement components for sensing point on 0° and 90°. In this figure, both u and w vanish, and the displacement only occurs in v. This means that only SH wave is excited, and A_0 and S_0 Lamb waves do not exist in these two directions. According to the wave group velocity, the displacement v can be also identified as the direct SH_0 waves, however their phases are

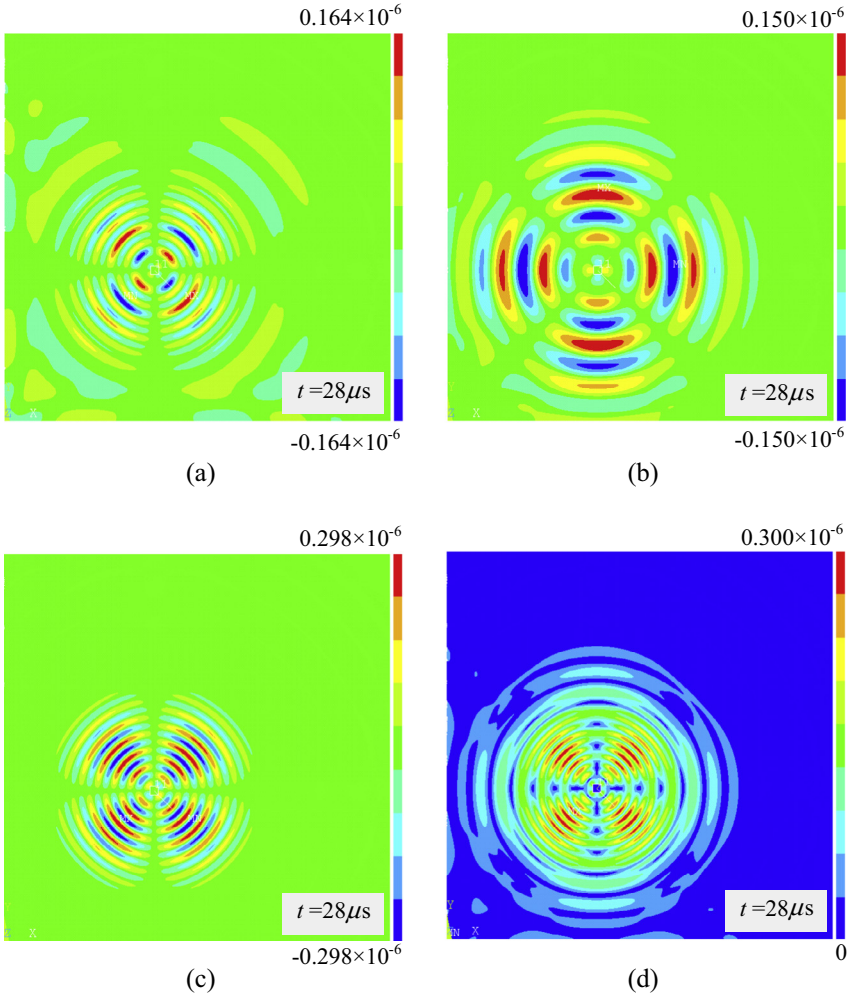

Fig. 4. Displacement contour in local coordinate under excitation of d_{36} type piezoelectric wafer: (a) displacement component u', (b) displacement component v', (c) displacement component w' and (d) total displacement.

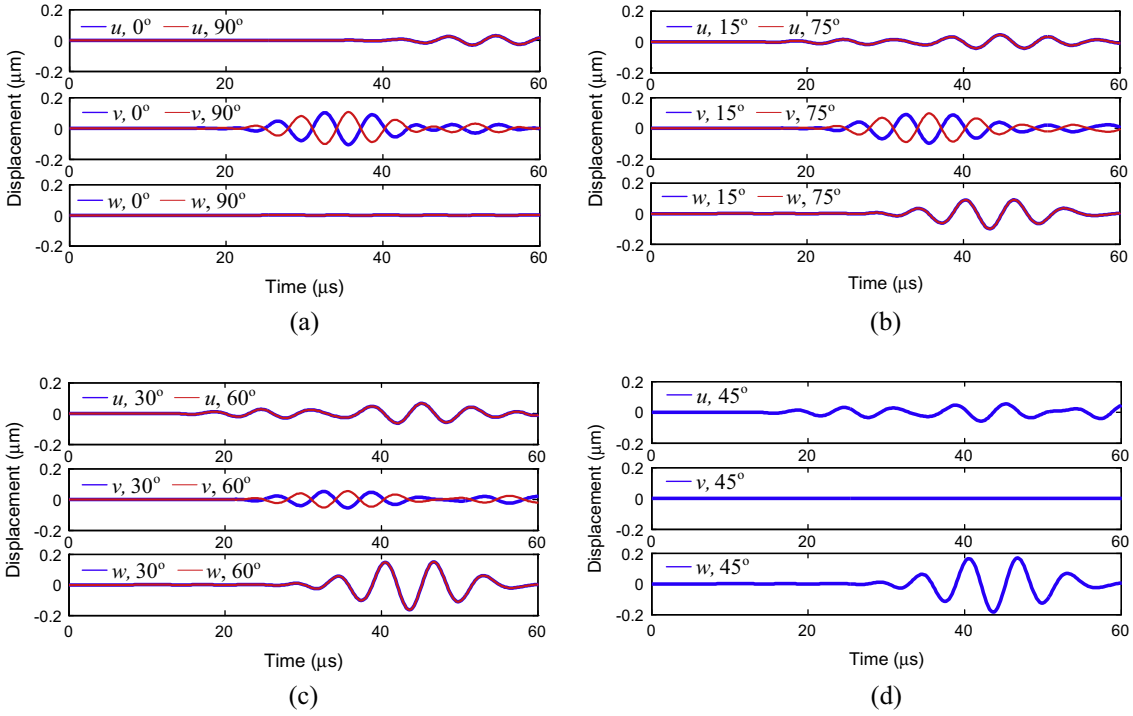

Fig. 5. Group velocity of Lamb wave and amplitude spectrum of excitation signal: (a) 0° and 90°, (b) 15° and 75°, (c) 30° and 60° and (d) 45°.

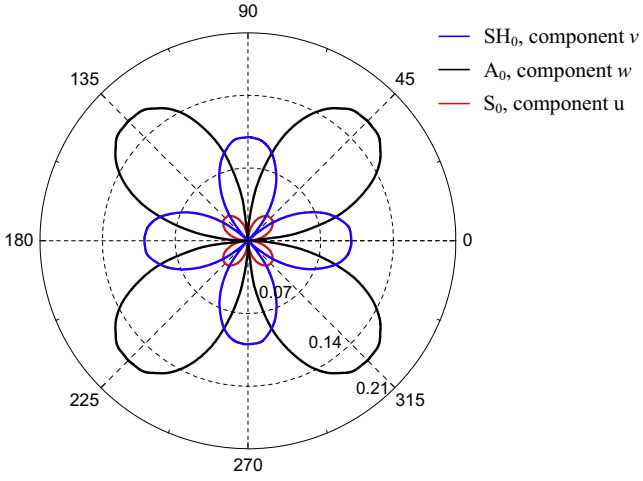

Fig. 6. Displacement amplitude versus direction of wave propagation for A_0, S_0, and SH_0 modes.

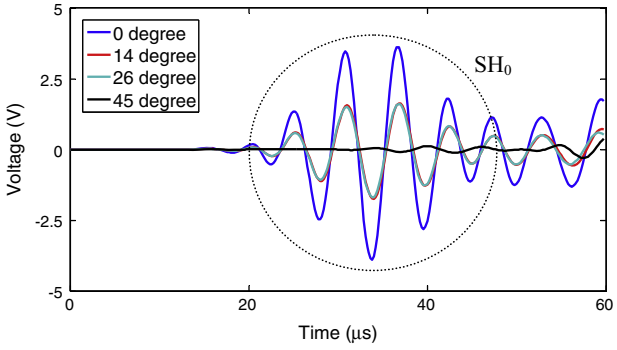

Fig. 8. Voltage responses of d_{36} type sensor to SH waves with different propagation directions.

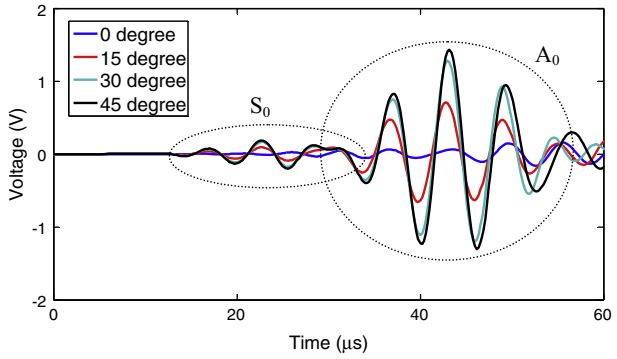

Fig. 7. Voltage responses of d_{36} type sensor to Lamb waves from different angles of wave propagation.

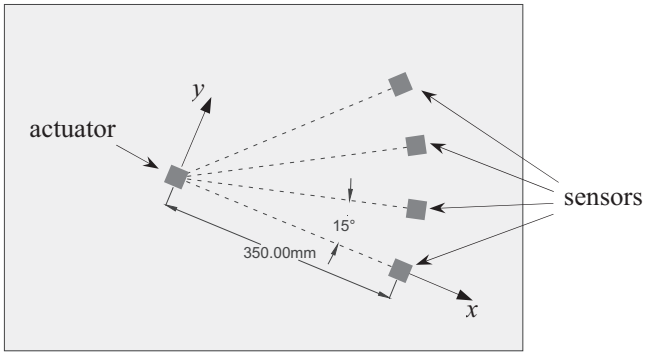

Fig. 9. Layout and location of piezoelectric wafers.

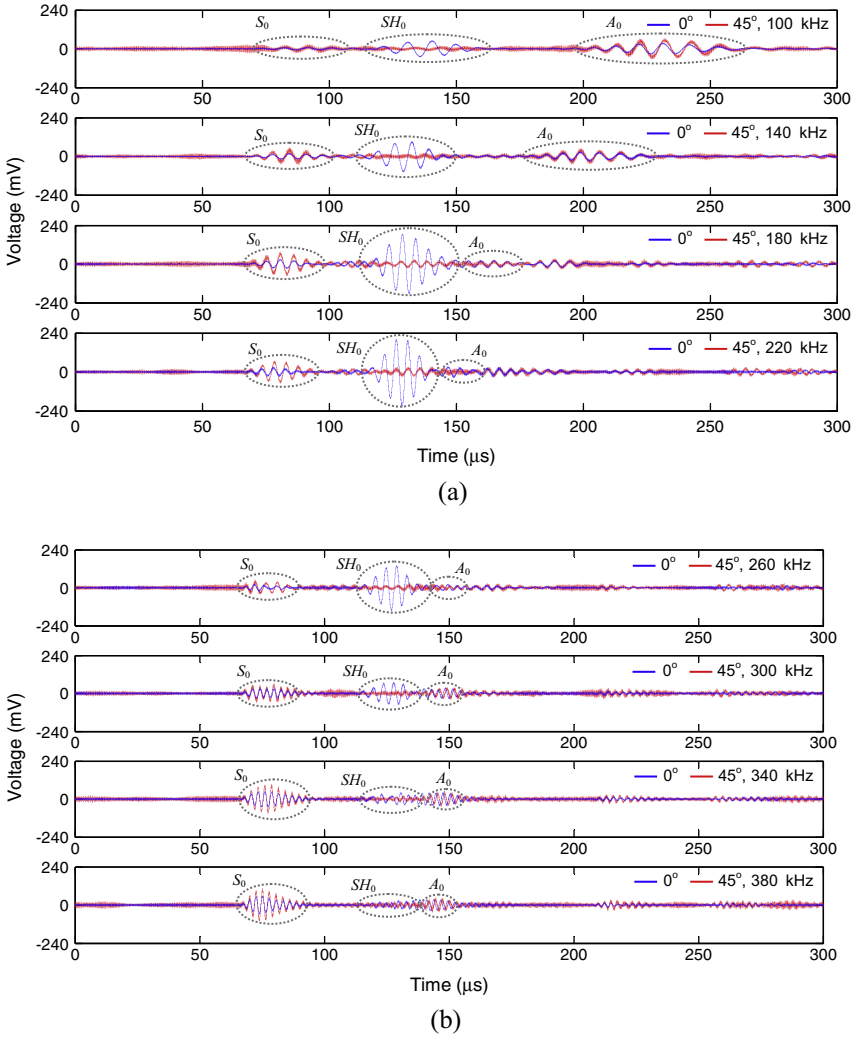

Fig. 10. Typical output voltage for different center frequencies at 0° and 45° in experiments: (a) 100–220 kHz and (b) 260–380 kHz.

opposite for 0° and 90°. In Fig. 5(b), the displacement v is smaller, and on the other two components, displacement responses are also obviously detected. Wave velocity indicates that they are A_0 and S_0 mode Lamb waves. For the sensing points on 30° and 60°, the amplitude of the SH wave becomes less and the A_0 and S_0 mode Lamb waves increase further. In Fig. 5(d), SH wave is unable to identified, while the other two modes Lamb waves reach their crest value in the amplitude.

Fig. 6 shows absolute values of the maximum amplitude of three displacement components versus the angle of wave propagation from 0° to 360°. According to the guided wave structure, v is the only component of SH_0 wave, and w and u are the dominant components of A_0 and S_0 wave, respectively. For SH_0, A_0 and S_0 wave modes, the amplitude curve is extracted at the time 26.8 μs, 31.2 μs and 15.2 μs respectively (they do not occur simultaneously). Due to the symmetry, the curves in the other three quadrants have the same shapes. It should be noted that the relative values among these three mode waves in this figure are only available at 160 kHz. With tuning frequencies, their relative values will change.

4.2. Guided waves detection using d_{36} type wafer

According to reciprocity principle, the voltage responses of d_{36} type sensor excited by the wave motion will also vary from different angles of wave propagation, since the d_{36} type transducer shows apparent directionality when it is used as actuator. Moreover, d_{36} type actuator is able to generate both Lamb and SH waves, thus the d_{36} type sensor is expected to detect above two types of guided waves. In this work, two simulations are set up to explore the voltage response of the d_{36} type sensor received from the waves coming from different angles.

For Lamb waves, a square d_{31} type piezoelectric wafer is used as actuator, four d_{36} type sensors are placed around it away the same distance, and their relative angle are 0°, 15°, 30° and 45°, respectively. Since the d_{31} type piezoelectric actuator is omnidirectional, above four sensors will incur the same wave motion. Fig. 7 shows the voltage responses for all sensors. d_{36} type sensor has maximum sensitivity on 45°, but minimum sensitivity on 0° for both A_0 and S_0 mode Lamb waves.

For investigating the response of d_{36} sensor to SH_0 wave, a square d_{36} type actuator is used to excite this non-dispersive wave. Four d_{36} type sensors are placed on 0°, 90°, 180° and 270° of the actuator to detect SH wave, but their relative angle to the actuator are 0°, 14°, 26° and 45°, respectively. These angles are selected due to the orthotropic grid in the finite element model.

Fig. 8 shows the results from this simulation. The maximum voltage output occurs at the 0°, and the minimum voltage output at the 45°. Since the square wafer covers a small area but not a point, the response at the 45° is not absolute zero.

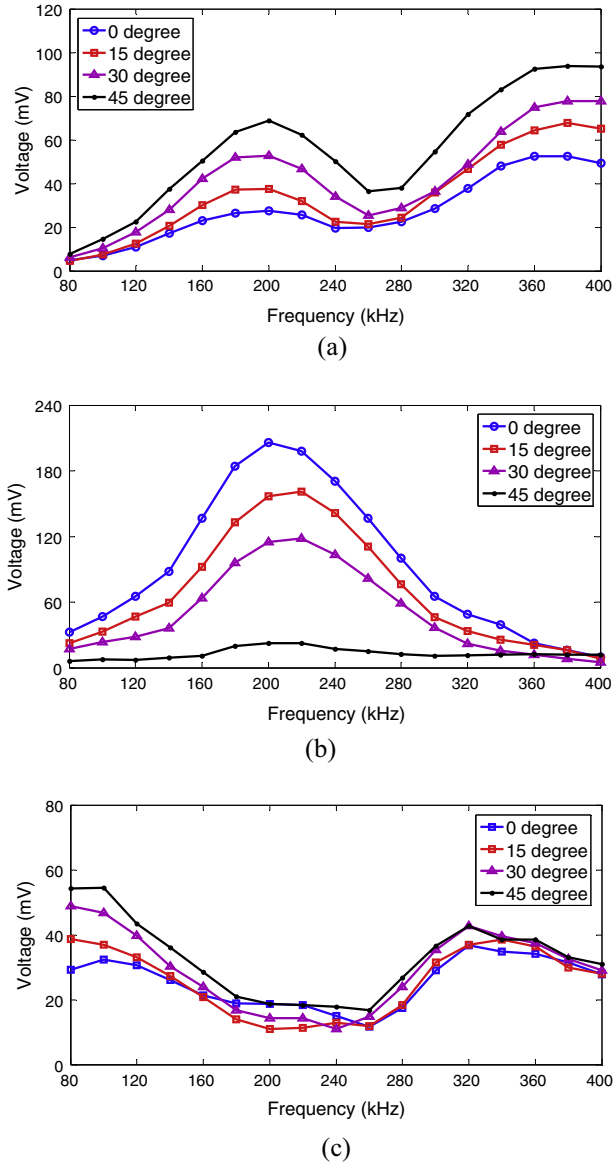

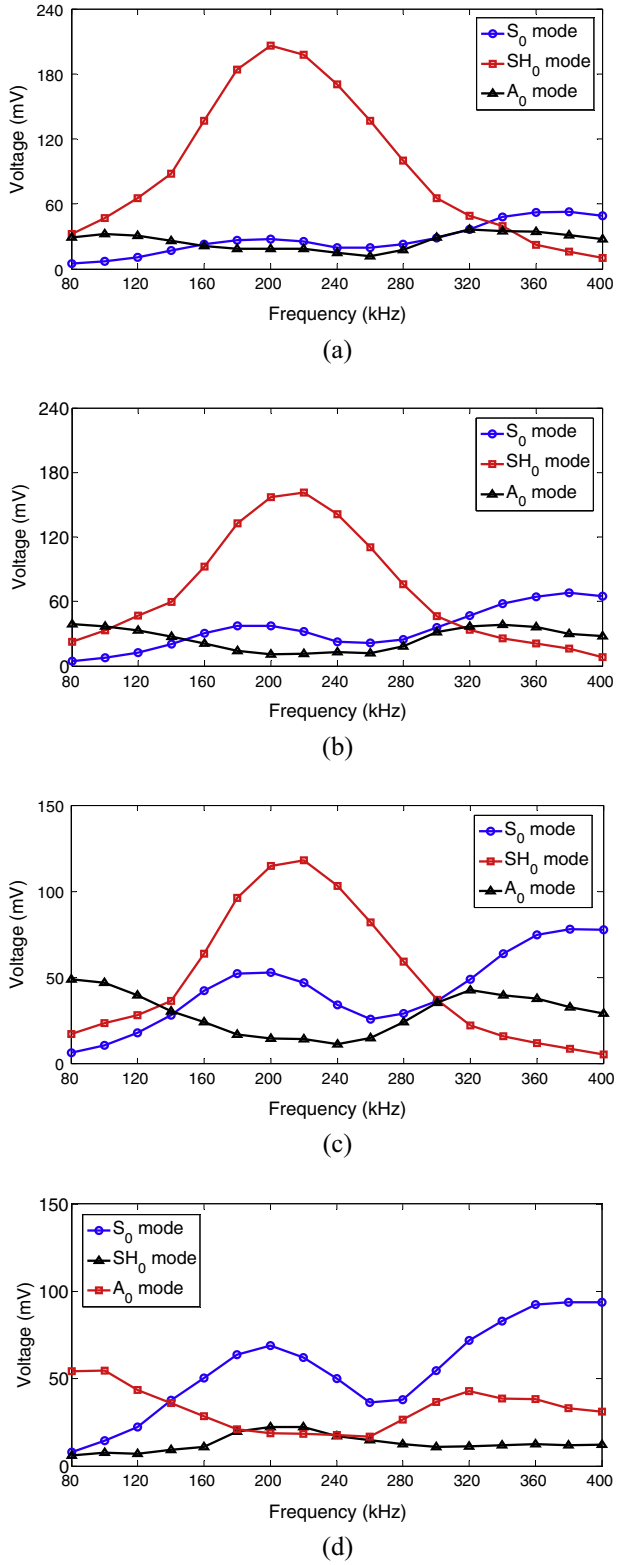

Fig. 11. Wave amplitude versus frequencies: (a) S_0 mode, (b) SH_0 mode and (c) A_0 mode.

Fig. 12. Wave amplitude versus frequencies: (a) 0°, (b) 15°, (c) 30° and (d) 45°.

5. Experimental investigations

5.1. Experimental setup

Experiments were designed to investigate not only the directionality of d_{36} type actuator and sensor, but also the amplitude sensitivity to frequency. Different from the simulations, in the experiments effects of d_{31} and d_{32} piezoelectric coefficients also can be considered. According to the results from FEM, three modes guided waves will be excited and propagate with their respective group velocities, thus the waves with higher velocity will reflect and overlap the waves with slower waves, which results in difficulty in amplitude analysis. Therefore, a large aluminum plate (1200 mm × 2400 mm × 1.0 mm) is used in the tests to extend the paths of wave reflections. Five d_{36} type wafers are mounted on the top surface of an aluminum plate. One of them is used as actuator, and the other four used as sensors are arranged around the actuator at 0°, 15°, 30° and 45° respectively. Their layout and location are shown in Fig. 9, in which the plate and wafers are not actual size. The distance between all wafers is 35 cm. The size of the wafers as both actuator and sensor is 7 mm × 7 mm × 0.5 mm. This thin wafer can reduce the effect of induced bending moment applied to the plate from the wafer. The super glue, which may form very thin and stiff adhesive layer, was used to attach these wafers on the plate. The actuator was driven by a function

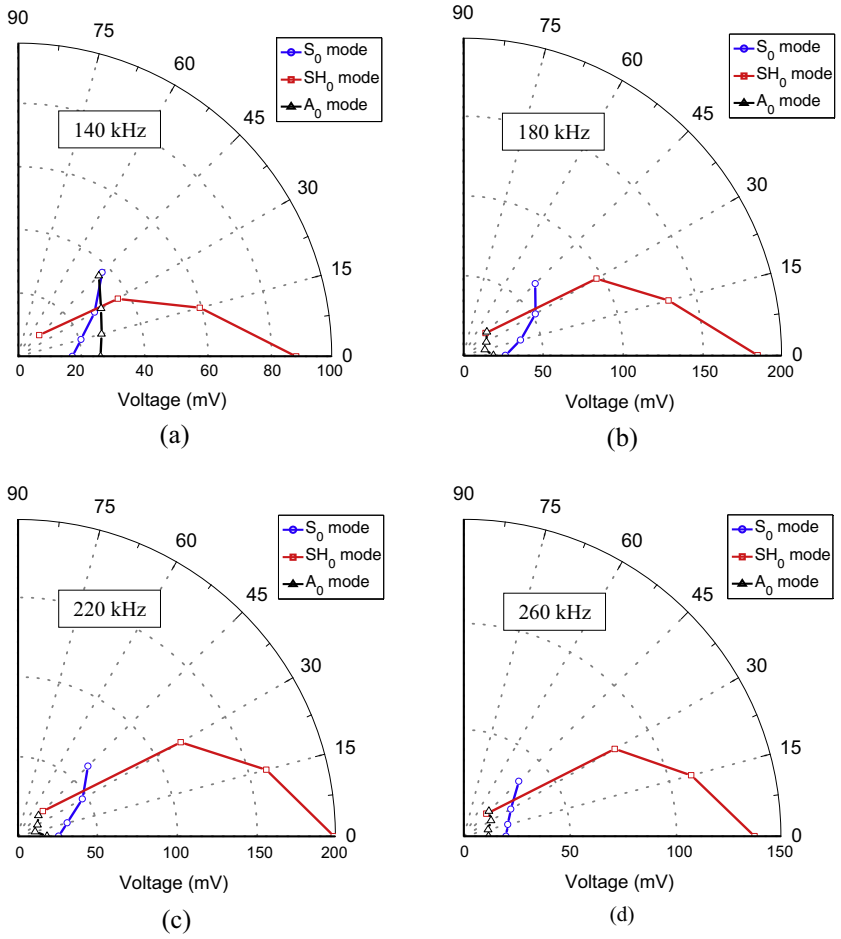

Fig. 13. Wave amplitude versus angle of wave propagation: (a) 140 kHz, (b) 180 kHz, (c) 220 kHz and (d) 260 kHz.

generator (AFG3252C, Tektronix, Inc.), into which a five-peaked wave signal was preprogrammed. Its amplitude and center frequency can be changed during the test. A wideband (DC-2 MHz) power amplifier (TEGAM 2350) was used to amplify excitation voltage. The signal induced from the sensor was collected directly with 2GS/s sampling rate by a digital oscilloscope (DPO 2024, Tektronix, Inc.). The center frequencies of excitation signal f_c is varied from 80 kHz to 400 kHz in increments of 20 kHz for all angles. According to the group velocities from Fig. 3, among these frequencies, overlapping hardly occurs for all three modes waves, so the reliable amplitudes are able to be obtained from the experimental results.

5.2. Amplitude versus frequency for all modes

The voltage responses of piezoelectric sensor vary as the exciting frequency sweeps. Since the experiments obtained a large number of data, only typical output voltage of sensors for different center frequencies at 0° and 45° is selected to be shown in Fig. 10, in which the amplitudes of excitation signals were kept fixed on V_{pp} = 2 V. The A_0, S_0 and SH_0 wave modes can be identified from experimental data according to group velocity. These curves show the varying amplitudes and effects of dispersion to A_0 and S_0 modes from lower to higher frequency. The waveforms obviously disperse due to wave dispersion characteristics.

All wave amplitudes with respect to frequencies for all wave modes are shown in Fig. 11. For comparison purpose, all data is also replotted according to angle of wave propagation in Fig. 12. It can be found that for different angles of wave propagation, the S_0, SH_0 and A_0 wave modes have the same tuning frequency characteristics, respectively, but for the same angle, the tuning frequency characteristics are different for these three modes. For S_0 mode, it reaches the first peak at 200 kHz, then decrease to the minimum around 260 kHz and then increase. For SH_0 mode, it reaches maximum value at around 200 kHz, then decrease monotonically. Additional tests indicate that the wave amplitude of the SH_0 mode does not increase again until 1020 kHz, therefore no more data is shown in this work. For A_0 mode, the wave amplitudes also vary with frequency. For the data from 0° direction, the SH_0 mode is dominant from about 160 kHz to 280 kHz. It can be expected that the SH_0 wave mode is easy to be distinguished in this frequency range. In addition, it seems that the data in Fig. 11(c) was affected by errors, which might be induced during amplitude identification for the dispersed wave forms.

5.3. Amplitude versus angle of wave propagation for all wave modes

Four excitation frequencies where the SH_0 mode is dominant are selected to show the amplitude variation with angles of wave propagation, shown in Fig. 13. For A_0 and S_0 modes, they still appear due to the existence of d_{31} and d_{32} piezoelectric coefficients. In addition, according to Fig. 13 the rates of amplitude change from 0° to 45° for SH_0 mode are various for different frequencies, but the

angles corresponding to maximum and minimum wave amplitudes are the same as those from simulation.

6. Conclusions

This paper examines the fundamental characteristics of a new d_{36} type piezoelectric transducer, made from a PMN–PT crystal. Specifically the tuning frequency characteristics and directionality for the piezoelectric wafer are investigated in application of guided waves generation and sensing. According to the guided wave theory, the SH_0 wave mode is a non-dispersive, which has many advantages for structural damage detection. The PMN–PT wafer has been demonstrated that it is capable of generating and detecting SH_0 wave mode. Due to its materials anisotropy, the SH_0 wave mode exhibits wave directionally. In the preliminarily FEM analyses, it proves above points based on the displacement components generated by the d_{36} type piezoelectric wafer, and then voltage responses show further that SH_0 wave mode is dominant at 0°, but negligible small at 45°; while the A_0 and S_0 wave mode show the reverse trend.

Experiments were conducted to investigate both the tuning frequency characteristics and wave mode directionality for the proposed wafer. Based on wave amplitudes obtained, the following conclusions are drawn:

(1) The A_0 and S_0 wave modes are affected greatly by dispersion; while the SH_0 wave mode maintains original waveform and constant group velocity with respect to varying frequencies.
(2) In the direction along 0°, SH_0 wave mode is dominant between about 160 kHz and 280 kHz, and then decreases gradually. Similar phenomena are observed for the other three directions. In the direction along 45°, SH_0 wave mode is hardly detected, whereas the A_0 and S_0 wave modes are mostly dominant. It indicates that among the specific frequency range, the proposed wafer can be used to generate and detect SH_0 wave in specific directions. With this property, the d_{36} type piezoelectric wafer is suited to be used in long structure for damage detection, because the other modes wave will become decrease in magnitude through long travel.
(3) Wave amplitudes of A_0 and S_0 wave modes in different directions have similar frequency tuning characteristic, but have different turning points from the PZT reported in the literature [10]. This is due to inherently different mechanical properties of piezoelectric wafer.

Acknowledgements

The financial support from the National Key Technology R&D Program under Grant No. 2011BAK02B02 & 2014BAG05B07, and the National Science Foundation of China under Grant No. 50908066 is gratefully appreciated.

References

[1] P. Cawley, D. Alleyne, The use of Lamb waves for the long range inspection of large structures, Ultrasonics 34 (1996) 287–290.
[2] A. Raghavan, C.E.S. Cesnik, Review of guided-wave structural health monitoring, Shock Vib. Dig. 39 (2007) 91–114.
[3] S. Rokhlin, Diffraction of Lamb waves by a finite crack in an elastic layer, J. Acoust. Soc. Am. 67 (1980) 1157–1165.
[4] S. Santhanam, R. Demirli, Reflection of Lamb waves obliquely incident on the free edge of a plate, Ultrasonics 53 (2013) 271–282.
[5] J.L. Rose, Ultrasonic Waves in Solid Media, Cambridge University Press, Cambridge, 2004.
[6] H. Kwun, C.M. Teller, Magnetostrictive generation and detection of longitudinal, torsional, and flexural waves in a steel rod, J. Acoust. Soc. Am. 96 (1994) 1202–1204.
[7] G.M. Light, H. Kwun, S.Y. Kim, R.L. Spinks Jr., Health monitoring of piping and plate using the Magnetostrictive Sensor (MsS) guided-wave technology, in: Proc. of 2nd Mid. E. NDT Conf. Exhib., Jubail Industrial City, Saudi Arabia, 2003.
[8] Z. Liu, C. He, B. Wu, X. Wang, S. Yang, Circumferential and longitudinal defect detection using T(0,1) mode excited by thickness shear mode piezoelectric elements, Ultrasonics 44 (2006) e1135–e1138.
[9] H.M. Seung, H.W. Kim, Y.Y. Kim, Development of an omni-directional shear-horizontal wave magnetostrictive patch transducer for plates, Ultrasonics 53 (2013) 1304–1308.
[10] V. Giurgiutiu, Lamb wave generation with piezoelectric wafer active sensors for structural health monitoring, in: Proc. SPIE. 5056, Smart Structures and Materials 2003: Smart Structures and Integrated Systems, 111 (August 5, 2003), http://dx.doi.org/10.1117/12.483492.
[11] W. Zhou, H. Li, F.-G. Yuan, Guided wave generation, sensing and damage detection using in-plane shear piezoelectric wafers, Smart Mater. Struct. 23 (2014) 015014, http://dx.doi.org/10.1088/0964-1726/23/1/015014.
[12] S. Zhang, W. Jiang, R.J. Meyer Jr., F. Li, J. Luo, W. Cao, Measurement of face shear properties in relaxor-$PbTiO_3$ single crystals, J. Appl. Phys. 110 (2011) 064106.